

Thermal stitching: Extending the reach of quantum fermion solvers

Justin C. Smith^{1,2} and Kieron Burke^{2,3}

¹*Department of Mathematics, University of California, Los Angeles, CA 90095*

²*Department of Physics and Astronomy, University of California, Irvine, CA 92697*

³*Department of Chemistry, University of California, Irvine, CA 92697*

(Dated: March 23, 2021)

For quantum fermion problems, many accurate solvers are limited by the temperature regime in which they can be usefully applied. The Mermin theorem implies the uniqueness of an effective potential from which both the exact density and free energy at a target temperature can be found, via a calculation at a different, reference temperature. We derive exact expressions for both the potential and the free energy in such a calculation, and introduce three controllable approximations that reduce the cost of such calculations. We illustrate the effective potential and its free energy, and test the approximations, on the asymmetric two-site Hubbard model at finite temperature.

The fermionic quantum problem occurs in many areas of physics and is notoriously difficult to solve[1]. It is at the heart of all electronic structure problems, and so solution methods have enormous impact in condensed matter physics, quantum chemistry, materials science, and beyond[2]. Over decades, many diverse approaches have been developed and refined[3]. In almost all cases, there are trade-offs between accuracy, computational cost, and domain of applicability. Some techniques are almost solely designed to work on finite systems at zero temperature (e.g., many ab initio quantum chemical approaches), while others are extremely general but costs become prohibitive as the temperature lowers (e.g., path integral Monte Carlo, PIMC[4, 5]). A collection of high-accuracy methods has recently been benchmarked on small strongly-correlated lattice models[6]. On the other hand density-functional methods are relatively inexpensive, but require an uncontrolled approximation to the exchange-correlation (XC) energy. Recently, density functional theory (DFT) methods have enjoyed considerable success in being applied at temperatures relevant to warm dense matter (WDM), a phase of matter with properties between those of solids and plasmas[7], such as occurs in fusion experiments and planetary cores[8–20].

The central question addressed in this work is: Is there some way that a quantum fermion solver could be run at one temperature (the reference temperature) to yield results at some other temperature (the target temperature)? Such a scheme could be applied to many diverse combinations of calculations. In the examples above, it could be used to bootstrap PIMC calculations to lower temperatures, quantum chemical calculations to finite temperatures, or to combine DFT methods with more accurate solvers for WDM[21–23].

We show that the answer is in principle yes, at least for extracting the free energy and density at the target temperature. Inspired by Ref. [24], we use the Mermin theorem[25] to define a unique effective one-body potential from which, with an accurate quantum solver, we can extract the target quantities. We derive the relevant formulas for a finite-temperature Kohn-Sham treatment. We identify three useful, controllable approximations that make extraction of the

target free energy easier in practice. Finally, we illustrate the relevant exact quantities and test the approximations on the finite-temperature asymmetric Hubbard dimer.

Although our formulas might be applied to any quantum fermion problem, we will discuss WDM simulations as a concrete example. Mermin generalized the Hohenberg-Kohn theorem[26] to systems in thermal equilibrium at non-zero temperatures[25]. Thermal DFT (thDFT) became a popular tool of plasma physics in subsequent decades[27–29]. The advent of accurate ground-state approximations and robust materials codes led to many recent successes of thDFT[12, 13, 18, 19, 30–35]. For greater reliability and in principle higher accuracy, but at much higher computational cost, path integral Monte Carlo (PIMC) simulations are used[4, 5, 36–40].

As in the ground state, thDFT is made computationally tractable by the use of a non-interacting potential $v_s^\tau(\mathbf{r})$ that yields the interacting density, $n^\tau(\mathbf{r})$, at temperature τ . This Mermin-Kohn-Sham (MKS) system is exact in principle but in practice requires approximations to the exchange-correlation (XC) free energy, $A_{\text{XC}}^\tau[n]$, as a functional of the density[41]. Most WDM simulations use the zero-temperature approximation (ZTA)[42], in which $A_{\text{XC}}^\tau[n]$ is replaced by $E_{\text{XC}}[n]$, an approximation to the ground state XC energy[43], but used in the thermal MKS equations. An alternative is to use the thermal local density approximation, where a parametrization of the XC free energy of the homogeneous electron gas is used to approximate $A_{\text{XC}}^\tau[n]$ [39, 44, 45]. Thermal generalized gradient approximations[46, 47] have also been suggested.

Begin with the Mermin-Kohn-Sham scheme. The equations are identical to those of the ground state,

$$\left\{ -\frac{1}{2}\nabla^2 + v_s^\tau(\mathbf{r}) \right\} \phi_i^\tau(\mathbf{r}) = \epsilon_i^\tau \phi_i^\tau(\mathbf{r}), \quad (1)$$

with the exception that the density is found by thermally occupying the MKS orbitals:

$$n^\tau(\mathbf{r}) = \sum_i f_i^\tau |\phi_i^\tau(\mathbf{r})|^2, \quad (2)$$

where the occupations are Fermi factors at temperature τ . $v_s(\mathbf{r})$ is defined by Eqs. (1) and (2). Write the free energy in terms of the MKS components:

$$A[v] = \min_n (T_s^\tau[n] - \tau S_s^\tau[n] + U[n] + A_{\text{xc}}^\tau[n] + \mathcal{I}[nv]), \quad (3)$$

where T_s^τ is the MKS non-interacting kinetic energy at temperature τ , S_s^τ is the corresponding entropy, U is the Hartree energy, and we have introduced

$$\mathcal{I}[f] = \int d^3r f(\mathbf{r}) \quad (4)$$

to represent the external potential energy. Writing

$$v_s^\tau(\mathbf{r}) = v(\mathbf{r}) + v_{\text{H}}[n](\mathbf{r}) + v_{\text{xc}}^\tau[n](\mathbf{r}), \quad (5)$$

and identifying $v_{\text{H}}(\mathbf{r})$ as the Hartree potential and $v_{\text{xc}}^\tau(\mathbf{r})$ as the functional derivative of A_{xc}^τ , the self-consistent solution of the MKS equations finds the minimum density in Eq. (3).

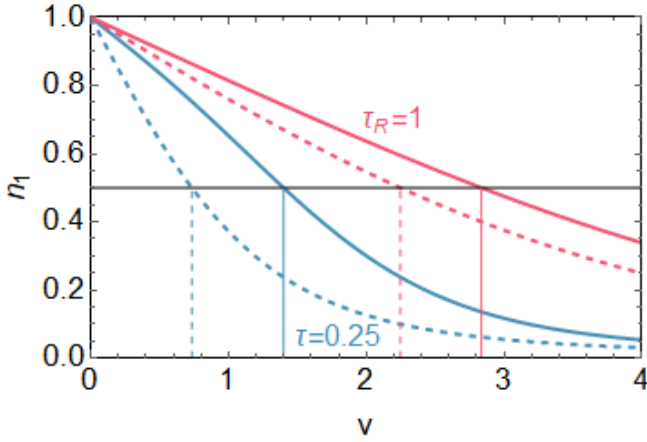


FIG. 1. n_1 vs. x at $\tau = 0.25$ (blue) and $\tau = 1$ (red). Solid lines are $U = 1$ and dashed are non-interacting, $U = 0$. The intersections with the horizontal line at $n_1 = 0.5$ give the v values that yield $n_1 = 0.5$ for the given temperature and interaction.

We make this more concrete with a simple model. The asymmetric Hubbard dimer has seen increasing use as an exact model to test and understand many flavors of DFT including ground state[48, 49], time-dependent[50–53], ensemble[54], thermal[42, 55], and DFT-like methods[56]. Its Hamiltonian is

$$\hat{H} = -t \sum_{\sigma} (\hat{c}_{1\sigma}^\dagger \hat{c}_{2\sigma} + \text{H.c.}) + \sum_i (U \hat{n}_{i\uparrow} \hat{n}_{i\downarrow} + v_i \hat{n}_i) \quad (6)$$

where $\hat{c}_{i\sigma}^\dagger$ ($\hat{c}_{i\sigma}$) is the electron creation (annihilation) operator and $\hat{n}_{i\sigma} = \hat{c}_{i\sigma}^\dagger \hat{c}_{i\sigma}$ is the number operator, t is the strength of electron hopping, U is the Coulomb repulsion, and v_i is the onsite potential. We choose $v_1 + v_2 = 0$, define $v = v_2 - v_1$, and $2t = 1$. In lattice DFT the site-occupations[57], n_1 and n_2 , are the analogs of the density.

We work at half-filling by setting $\langle N \rangle = 2$ which restricts $\mu = U/2$ to maintain particle-hole symmetry. Fig. 1 shows exact thermal calculations. The solid red line is the density on site 1 as a function of the onsite potential v , for a relatively hot temperature ($\tau = 1$). The Mermin theorem guarantees its monotonicity. The dashed red line is the same map but for tight-binding, i.e., $U = 0$. Thus, for a system with $v = 2.834$ (marked by solid red vertical line), $n = 0.5$ at $\tau = 1$. The MKS potential is $v_s^\tau = 2.246$ (vertical dashed red line), and the difference is the HXC contribution. The blue lines denote the same things at a lower temperature, $\tau = 1/4$.

The logical basis of the MKS scheme is the Mermin theorem. Mermin proved that in the grand canonical ensemble for fixed temperature and chemical potential there exists a one-to-one correspondence between the external potential and electronic density for given particle statistics, interaction, and temperature, τ [25]. Assuming v -representability, the map $\bar{n}^\tau[v](\mathbf{r})$ is invertible and the map $v^\tau[n](\mathbf{r})$ exists. Note that the former is a potential functional (denoted by a bar), while the latter is a density functional. Assuming non-interacting representability, we may then write

$$\bar{v}_s^\tau[v](\mathbf{r}) = (n_s^\tau)^{-1}[\bar{n}^\tau[v]](\mathbf{r}). \quad (7)$$

This compact expression is the map between the one-body potential of the interacting problem and its KS alter ego, i.e., this is the KS potential as a functional of the one-body potential of the interacting problem, which is different from its density dependence as expressed in Eq. (5).

For any system, we can define an effective thermal potential, $\bar{v}_{\tau R}^\tau(\mathbf{r})$, as the one-body potential that yields the exact density at τ by performing a calculation at τ_R . This is unique by Mermin's theorem and can be written

$$\bar{v}_{\tau R}^\tau[v](\mathbf{r}) = (n^{\tau R})^{-1}[n^\tau[v]](\mathbf{r}). \quad (8)$$

A non-interacting map is defined in the same way. Figure 1 also illustrates the effective thermal potential logic. The horizontal line is $n_1 = 0.5$ and everywhere that it intersects a curve corresponds to the potential that yields $n_1 = 0.5$ for the given temperature and interaction strength. Thus $\bar{v}_{\tau R}^\tau[v]$ is given by the dependence of the blue vertical line on the red one, with an analogous non-interacting version with dashed vertical lines. This effective potential has some specific symmetry properties, namely

$$\bar{v}_{\tau R}^\tau[\bar{v}_{\tau R}^{\tau R}[v]](\mathbf{r}) = \bar{v}_\tau^\tau[v](\mathbf{r}) = v(\mathbf{r}). \quad (9)$$

We now wish to derive the effective thermal potential for an MKS calculation, using some $\tilde{v}_{\text{xc}}^\tau[n](\mathbf{r})$, where this XC potential could be either approximate or exact. To do this, we must use the concept of a ffunctional[58]. A functional is a function of a function, whereas a ffunctional is a functional of a functional. Identify $n^\tau\{\tilde{v}_{\text{xc}}\}[v](\mathbf{r})$ as the density at temperature τ found by solving the MKS equations with $\tilde{v}_{\text{xc}}^\tau[n](\mathbf{r})$. Then

$$\bar{v}_{\tau R}^{\tau R}[v](\mathbf{r}) = v_s^{\tau R}[n^\tau\{\tilde{v}_{\text{xc}}\}[v]](\mathbf{r}) - v_{\text{HXC}}^{\tau R}[n^\tau\{\tilde{v}_{\text{xc}}\}[v]](\mathbf{r}). \quad (10)$$

This result shows how to construct an approximate effective thermal potential from a MKS calculation at two different temperatures with a given XC free energy potential. Simply calculate the density from MKS at the desired temperature, find what non-interacting potential yields that density at the reference temperature, and subtract off the approximate HXC potential evaluated at the reference temperature. In Fig. 1, the first term is the MKS contribution (vertical dashed blue line), while the second is the HXC correction (difference between solid and dashed vertical blue lines). Thus a DFT approximation might be used to generate PIMC-quality densities at τ by performing PIMC calculations only at τ_R . Our result satisfies several important conditions: (i) if the exact XC functional is used, the exact $n^\tau(\mathbf{r})$ is found; (ii) if an approximate XC is used, and the resulting effective thermal potential is used in a MKS calculation with the same XC approximation, the corresponding self-consistent approximate density is found; (iii) if the temperatures are set equal, the exact result is recovered. But the symmetry of Eq. (9) is lost with an approximate XC.

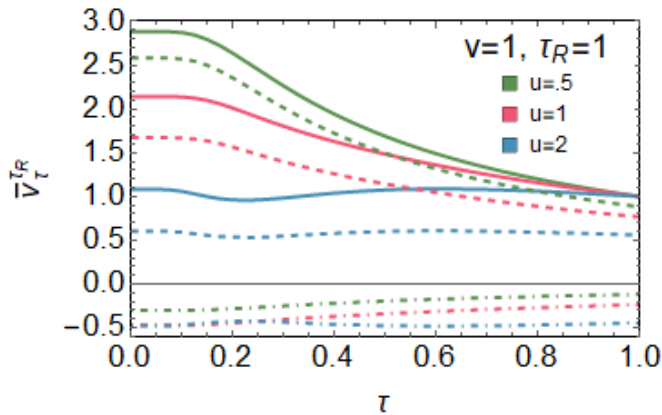


FIG. 2. Effective thermal potential for $v = 1$ and $\tau_R = 1$ for various correlation strengths. Solid curves are interacting, dashed are non-interacting, and dot-dashed is Hxc. All calculations yield $\bar{v}_{\text{Hxc},\tau}^{\tau_R} \leq 0$.

In Fig. 2, we plot the exact effective thermal potential, for a system with $v = 1$. Green denotes weak correlation ($u = 0.5$). (In the ground state for $v = 0$, the radius of convergence of the small- u expansion is 2). The solid line is the interacting curve, which varies strongly with temperature (but approaches v as $\tau \rightarrow \tau_R$, as required). The dashed line is the MKS effective thermal potential, which mimics the interacting curve closely, and approaches the MKS potential at τ_R . The dot-dashed line is the HXC contribution, which is relatively small and much smoother, suggesting it might be amenable to approximation.

We also show what happens as we increase the correlation to $u = 1$ (red) and $u = 2$ (blue). For moderate correlation, the effects are similar, but larger. But for strong correlation temperature dependence is mitigated, the HXC contribution is comparable to the MKS piece, and small errors in its

approximation are less likely to be forgiven.

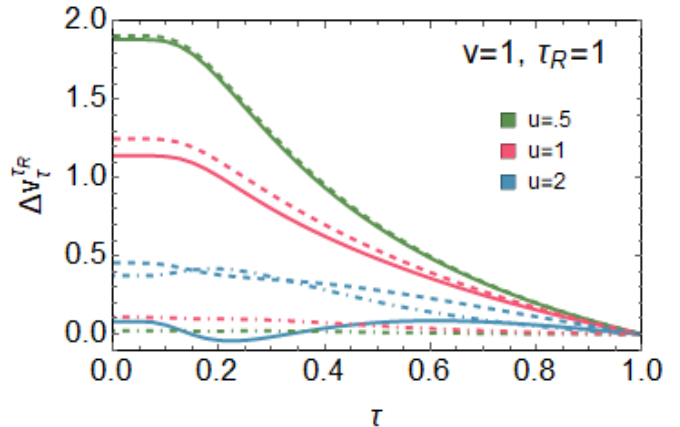


FIG. 3. Same as previous figure, but now for the difference between effective thermal potential and its reference.

In Fig. 3, we plot the difference between the effective thermal potential and its reference value (v and v_s^τ for interacting and non-interacting, respectively), showing that the HXC contributions are now even smaller. They remain monotonic when correlation is weak or moderate, and vanish rapidly as $\tau \rightarrow \tau_R$. This strongly suggests that approximating the XC contribution to the thermal correction potential with a local or semilocal density functional approximation should introduce relatively little error in the density for weakly correlated systems. For strong correlation, the HXC contribution is of the same order as the MKS potential, develops nonmonotonic behavior, and vanishes much more slowly with temperature. A semilocal density approximation might introduce much larger errors in this case.

Although the density is important, greatest interest is often in the free energy and related properties. Thus we need to generate accurate free energies from our formulas. We begin with a recently proven formula[59] in potential functional theory (PFT)[58, 60, 61] to calculate the free energy. In Ref. [59] PFT is generalized to the grand canonical ensemble. Assume the energy components are known exactly for some given reference potential, v_0 , and write $v^\lambda(\mathbf{r}) = v_0(\mathbf{r}) + \lambda\Delta v(\mathbf{r})$, where $\Delta v(\mathbf{r}) = v(\mathbf{r}) - v_0(\mathbf{r})$. The free energy of the system is then:

$$A^\tau[v] = A_0^\tau + \mathcal{I}[\bar{n}^\tau[v, \Delta v]\Delta v], \quad (11)$$

where $\bar{n}^\tau[v, \Delta v] = \int_0^1 d\lambda n^\tau[v^\lambda](\mathbf{r})$. Here 0 subscripts denote quantities for the reference potential. We find, exactly, for the deviation from the reference A_{HXC}^τ :

$$\begin{aligned} \Delta A_{\text{HXC}}^\tau[\Delta v] &= \mathcal{I}[\bar{n}^\tau[v, \Delta v]\Delta v] - \mathcal{I}[\bar{n}_s^\tau[v_s^\tau, \Delta v_s^\tau]\Delta v_s^\tau] \\ &\quad + \mathcal{I}[n^\tau[v]v_{\text{HXC}}^\tau - n_0^\tau[v_0]v_{\text{HXC},0}^\tau]. \end{aligned} \quad (12)$$

The derivation of Eq. (12) is given in the Supplemental Material[62].

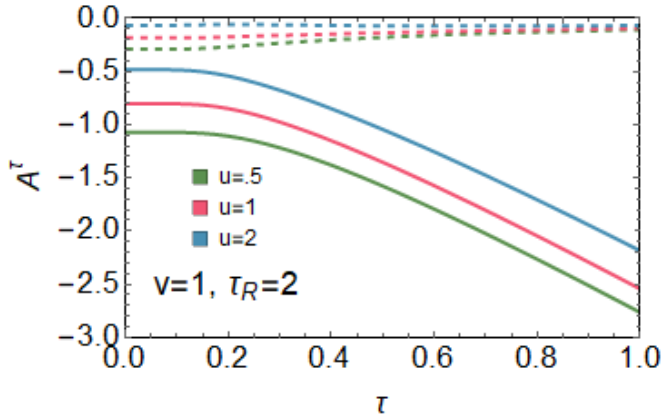


FIG. 4. Temperature dependence of the free energy and its deviation from reference for the same systems as in the previous figures.

To illustrate the value of a well-chosen reference, in Fig. 4, we plot the free energy versus temperature using Eq. (11) with the reference potential set to 0, i.e., the perfectly symmetric case. We see that the deviation from the reference is an order of magnitude smaller than the reference value, making it easier to approximate. Note that here our reference temperature is twice as high as before, but even at half its value, the deviation in the free energy from the reference is difficult to detect.

In principle, Eq. (12) is sufficient to extract the free energy from a thermal-stitching calculation. Although the input densities are required at the target temperature τ , these can all be found from calculations at the reference temperature. The last term in Eq. (12) is straightforward, but the first involves averages over λ that are cumbersome since the effective thermal potential must be evaluated for every λ . The last step in our work is to derive a controlled approximation that yields an accurate expression using only quantities evaluated at τ_R .

We make three distinct approximations. In the first, we note that the exact formula requires finding $n_s^\tau[v_{s,0} + \lambda\Delta v_s](\mathbf{r})$ which, in general, is not equal to $n^\tau[v_0 + \lambda\Delta v](\mathbf{r})$. However, they match at $\lambda = 0$ and $\lambda = 1$, and nearly agree everywhere for weak interaction, so we expect

$$n_s^\tau[v_{s,0} + \lambda\Delta v_s](\mathbf{r}) \approx n^\tau[v_0 + \lambda\Delta v](\mathbf{r}) \quad (13)$$

to produce very little error. A second approximation is to approximate each coupling-constant integral by a two-point formula:

$$\bar{n}^\tau[v, \Delta v](\mathbf{r}) \approx \frac{1}{2}(n^\tau[v_0](\mathbf{r}) + n^\tau[v](\mathbf{r})). \quad (14)$$

With these Eq. (12) greatly simplifies to

$$\Delta A_{XC}^{\tau, \text{app}}[v] = \mathcal{I}[(n^\tau[v] - \bar{n}^\tau[v])v_{XC}^\tau] - \mathcal{I}[(n^\tau[v_0] - \bar{n}^\tau[v])v_{XC,0}^\tau], \quad (15)$$

with the Hartree contributions explicitly canceling on both sides (See Supplemental Material for derivation[62]). Inserting the effective thermal potential is now simple:

$$\Delta A_{XC}^{\tau, \text{app}}[v] = \mathcal{I}[(n^{\tau_R}[\tilde{v}_\tau^{\tau_R}[v]] - \bar{n}^{\tau_R}[\tilde{v}_\tau^{\tau_R}[v]])v_{XC}^\tau] - \mathcal{I}[(n^{\tau_R}[\tilde{v}_\tau^{\tau_R}[v_0]] - \bar{n}^{\tau_R}[\tilde{v}_\tau^{\tau_R}[v]])v_{XC,0}^\tau]. \quad (16)$$

This formula yields (approximately) the XC free energy at τ using only densities from τ_R , effective thermal potentials, and the XC potential at τ , which can be extracted via a MKS inversion from the accurate density at τ , i.e. Eq. (7), and subtraction of the external and Hartree potentials.

Although Eq. (16) contains only quantities evaluated at the reference temperature, as required, they are awkward because the reference potentials and densities must be found for many values of λ , and then averaged over the coupling constant. This process can be simplified by a linear approximation for the thermal effective potential:

$$\begin{aligned} \tilde{v}_\tau^{\tau_R}[v^\lambda](\mathbf{r}) &= \tilde{v}_\tau^{\tau_R}[v_0 + \lambda(v - v_0)](\mathbf{r}) \\ &\approx \tilde{v}_\tau^{\tau_R}[v_0](\mathbf{r}) + \lambda(\tilde{v}_\tau^{\tau_R}[v](\mathbf{r}) - \tilde{v}_\tau^{\tau_R}[v_0](\mathbf{r})) \end{aligned} \quad (17)$$

which should be an excellent approximation for weak correlation.

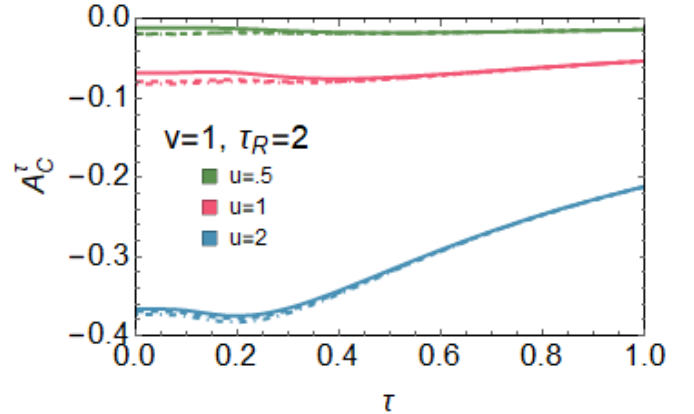


FIG. 5. Correlation free energy from effective thermal potential for the same system as previous figures. Solid is exact, dashed is from Eq. (16), and dot-dashed includes the further approximation of Eq. (17).

In Fig. 5, we plot correlation energies exactly, approximately but doing the coupling-integral in Eq. (16) explicitly, and approximately but with Eq. (17) to approximate the coupling-integrations. Using Eq. (16) introduces small errors for low temperatures but these quickly diminish as temperature increases. Interestingly, they seem no worse when correlations are stronger. Linearizing the potential slightly worsens the results, but makes a smaller error than already present in Eq. (16). This error also diminishes rapidly with increasing temperature. As noted in Ref. [42], correlation becomes a relatively smaller part of the total free energy as temperature increases. The majority of the contribution to the correlation free energy is in the reference term with

similar behavior in the correction term as seen for the total free energy, and we are making only a small error in approximating the correction.

In this work we have presented a formally exact method for determining electronic properties at temperature τ using a calculation at temperature τ_R . To do so, we defined an effective thermal potential which yields the exact density at τ of a given system. We have illustrated the effective thermal potential using the asymmetric Hubbard dimer. We have also derived an approximate formula from potential functional theory for the exchange-correlation free energy that uses only the effective thermal potential. We applied simple approximations to this equation to put it in a more elegant form and to make it only require the effective thermal potential.

We conclude with suggestions for approximations and future work. For extended matter in WDM simulations, an obvious reference potential is the uniform electron gas with the average electronic density of the entire system. The free energy of this system is (relatively) well known [23, 44, 45, 63, 64]. Then the coupling-constant integral connects local differences in the potential from its average value. Eq. (10) would also be first tested with e.g., a zero-temperature GGA approximation for the MKS approximation. This yields an approximate density at τ and the corresponding HXC approximation at τ_R . Then the same MKS code could be used to find the corresponding MKS potential at τ_R , by using any one of several feedback schemes to adjust $v_s^{\tau_R}(\mathbf{r})$ until the one yielding $\tilde{n}^\tau(\mathbf{r})$ is found. These then yield the approximation to the effective thermal potential to be used in an accurate quantum solver at τ_R . Note that one could also imagine this as the first step in an iterative procedure in which the output approximate density at τ is used in place of the MKS approximate density. This would unbalance the use of DFT in the formula which might in fact worsen the results. Only practical calculations can tell. Additional future tests and demonstrations of this theory include long Hubbard chains, more complicated lattices, and atoms. These tests can further show the theory's applicability and accuracy.

The authors acknowledge support from the US Department of Energy (DOE), Office of Science, Basic Energy Sciences under Award No. DE-FG02-08ER46496. J.C.S. acknowledges support through the NSF Graduate Research fellowship program under Award No. DGE-1321846.

-
- [1] P. A. M. Dirac, "Quantum mechanics of many-electron systems," *Proceedings of the Royal Society of London. Series A, Containing Papers of a Mathematical and Physical Character* **123**, 714–733 (1929).
- [2] Aurora Pribram-Jones, David A. Gross, and Kieron Burke, "Dft: A theory full of holes?" *Annual Review of Physical Chemistry* **66**, 283–304 (2015).
- [3] Richard M Martin, Lucia Reining, and David M Ceperley,

- Interacting Electrons* (Cambridge University Press, 2016).
- [4] D. M. Ceperley, "Path integrals in the theory of condensed helium," *Rev. Mod. Phys.* **67**, 279–355 (1995).
- [5] K. P. Driver and B. Militzer, "All-electron path integral monte carlo simulations of warm dense matter: Application to water and carbon plasmas," *Phys. Rev. Lett.* **108**, 115502 (2012).
- [6] Mario Motta, David M. Ceperley, Garnet Kin-Lic Chan, John A. Gomez, Emanuel Gull, Sheng Guo, Carlos A. Jiménez-Hoyos, Tran Nguyen Lan, Jia Li, Fengjie Ma, Andrew J. Millis, Nikolay V. Prokof'ev, Ushnish Ray, Gustavo E. Scuseria, Sandro Sorella, Edwin M. Stoudenmire, Qiming Sun, Igor S. Tupitsyn, Steven R. White, Dominika Zgid, and Shiwei Zhang (Simons Collaboration on the Many-Electron Problem), "Towards the solution of the many-electron problem in real materials: Equation of state of the hydrogen chain with state-of-the-art many-body methods," *Phys. Rev. X* **7**, 031059 (2017).
- [7] Frank Graziani, Michael P. Desjarlais, Ronald Redmer, and Samuel B. Trickey, eds., *Frontiers and Challenges in Warm Dense Matter*, Lecture Notes in Computational Science and Engineering, Vol. 96 (Springer International Publishing, 2014).
- [8] Balazs F Rozsnyai, James R Albritton, David A Young, Vijay N Sonnad, and David A Liberman, "Theory and experiment for ultrahigh pressure shock huginiots," *Physics Letters A* **291**, 226–231 (2001).
- [9] A. Höll, R. Redmer, G. Röpke, and H. Reinholz, "X-ray thomson scattering in warm dense matter," *The European Physical Journal D - Atomic, Molecular, Optical and Plasma Physics* **29**, 159–162 (2004).
- [10] S. H. Glenzer, O. L. Landen, P. Neumayer, R. W. Lee, K. Widmann, S. W. Pollaine, R. J. Wallace, G. Gregori, A. Höll, T. Bornath, R. Thiele, V. Schwarz, W.-D. Kraeft, and R. Redmer, "Observations of plasmons in warm dense matter," *Phys. Rev. Lett.* **98**, 065002 (2007).
- [11] E Garcia Saiz, Gianluca Gregori, Dirk O Gericke, Jan Vorberger, B Barbrel, RJ Clarke, Robert R Freeman, SH Glenzer, FY Khattak, M Koenig, *et al.*, "Probing warm dense lithium by inelastic x-ray scattering," *Nature Physics* **4**, 940–944 (2008).
- [12] André Kietzmann, Ronald Redmer, Michael P. Desjarlais, and Thomas R. Mattsson, "Complex behavior of fluid lithium under extreme conditions," *Phys. Rev. Lett.* **101**, 070401 (2008).
- [13] Winfried Lorenzen, Bastian Holst, and Ronald Redmer, "Demixing of hydrogen and helium at megabar pressures," *Phys. Rev. Lett.* **102**, 115701 (2009).
- [14] U.S. Department of Energy, *Basic Research Needs for High Energy Density Laboratory Physics: Report of the Workshop on High Energy Density Laboratory Physics Research Needs*, Tech. Rep. (Office of Science and National Nuclear Security Administration, 2009).
- [15] Ralph Ernstorfer, Maher Harb, Christoph T Hebeisen, Germán Sciaini, Thibault Dartigalongue, and RJ Dwayne Miller, "The formation of warm dense matter: experimental evidence for electronic bond hardening in gold," *Science* **323**, 1033–1037 (2009).
- [16] El Moses, RN Boyd, BA Remington, CJ Keane, and R Al-Ayat, "The national ignition facility: Ushering in a new age for high energy density science," *Physics of Plasmas* **16**, 041006 (2009).
- [17] FM Bieniosek, JJ Barnard, Alex Friedman, Enrique Heneostroza, Jin-Young Jung, MA Leitner, Steve Lidia, BG Logan,

- RM More, PA Ni, *et al.*, “Ion-beam-driven warm dense matter experiments,” in *Journal of Physics: Conference Series*, Vol. 244 (IOP Publishing, 2010) p. 032028.
- [18] Seth Root, Rudolph J. Magyar, John H. Carpenter, David L. Hanson, and Thomas R. Mattsson, “Shock compression of a fifth period element: Liquid xenon to 840 GPa,” *Phys. Rev. Lett.* **105**, 085501 (2010).
- [19] R F Smith, J H Eggert, R Jeanloz, T S Duffy, D G Braun, J R Patterson, R E Rudd, J Biener, A E Lazicki, A V Hamza, J Wang, T Braun, L X Benedict, P M Celliers, and G W Collins, “Ramp compression of diamond to five terapascals,” *Nature* **511**, 330–3 (2014).
- [20] LB Fletcher, HJ Lee, T Döppner, E Galtier, B Nagler, P Heimann, C Fortmann, S LePape, T Ma, M Millot, *et al.*, “Ultrabright x-ray laser scattering for dynamic warm dense matter physics,” *Nature Photonics* **9**, 274–279 (2015).
- [21] B. Militzer, “Path integral monte carlo and density functional molecular dynamics simulations of hot, dense helium,” *Phys. Rev. B* **79**, 155105 (2009).
- [22] K. P. Driver and B. Militzer, “First-principles simulations and shock hughoniot calculations of warm dense neon,” *Phys. Rev. B* **91**, 045103 (2015).
- [23] T. Schoof, S. Groth, J. Vorberger, and M. Bonitz, “*Ab Initio* thermodynamic results for the degenerate electron gas at finite temperature,” *Phys. Rev. Lett.* **115**, 130402 (2015).
- [24] M. W. C. Dharma-Wardana and F. Perrot, “Simple classical mapping of the spin-polarized quantum electron gas: Distribution functions and local-field corrections,” *Phys. Rev. Lett.* **84**, 959 (2000).
- [25] N. D. Mermin, “Thermal properties of the inhomogeneous electron gas,” *Phys. Rev.* **137**, A: 1441 (1965).
- [26] P. Hohenberg and W. Kohn, “Inhomogeneous electron gas,” *Phys. Rev.* **136**, B864–B871 (1964).
- [27] MWC Dharma-Wardana and R Taylor, “Exchange and correlation potentials for finite temperature quantum calculations at intermediate degeneracies,” *Journal of Physics C: Solid State Physics* **14**, 629 (1981).
- [28] MWC Dharma-Wardana and Francois Perrot, “Density-functional theory of hydrogen plasmas,” *Phys. Rev. A* **26**, 2096–2104 (1982).
- [29] Francois Perrot and M. W. C. Dharma-Wardana, “Exchange and correlation potentials for electron-ion systems at finite temperatures,” *Phys. Rev. A* **30**, 2619–2626 (1984).
- [30] Thomas R. Mattsson and Michael P. Desjarlais, “Phase diagram and electrical conductivity of high energy-density water from density functional theory,” *Phys. Rev. Lett.* **97**, 017801 (2006).
- [31] M. D. Knudson, M. P. Desjarlais, A. Becker, R. W. Lemke, K. R. Cochrane, M. E. Savage, D. E. Bliss, T. R. Mattsson, and R. Redmer, “Direct observation of an abrupt insulator-to-metal transition in dense liquid deuterium,” *Science* **348**, 1455–1460 (2015).
- [32] M. D. Knudson and M. P. Desjarlais, “Shock compression of quartz to 1.6 TPa: Redefining a pressure standard,” *Phys. Rev. Lett.* **103**, 225501 (2009).
- [33] M. D. Knudson, M. P. Desjarlais, and A. Pribram-Jones, “Adiabatic release measurements in aluminum between 400 and 1200 gpa: Characterization of aluminum as a shock standard in the multimegabar regime,” *Phys. Rev. B* **91**, 224105 (2015).
- [34] Bastian Holst, Ronald Redmer, and Michael P. Desjarlais, “Thermophysical properties of warm dense hydrogen using quantum molecular dynamics simulations,” *Phys. Rev. B* **77**, 184201 (2008).
- [35] SM Wahl, WB Hubbard, B Militzer, T Guillot, Y Miguel, N Movshovitz, Y Kaspi, R Helled, D Reese, E Galanti, *et al.*, “Comparing jupiter interior structure models to juno gravity measurements and the role of a dilute core,” *Geophysical Research Letters* (2017).
- [36] B. Militzer and D. M. Ceperley, “Path integral monte carlo calculation of the deuterium hughoniot,” *Phys. Rev. Lett.* **85**, 1890–1893 (2000).
- [37] V S Filinov, M Bonitz, W Ebeling, and V E Fortov, “Thermodynamics of hot dense h-plasmas: path integral monte carlo simulations and analytical approximations,” *Plasma Physics and Controlled Fusion* **43**, 743 (2001).
- [38] T. Schoof, M. Bonitz, A. Filinov, D. Hochstuhl, and J.W. Dufty, “Configuration path integral monte carlo,” *Contributions to Plasma Physics* **51**, 687–697 (2011).
- [39] Tobias Dornheim, Simon Groth, Travis Sjostrom, Fionn D. Malone, W. M. C. Foulkes, and Michael Bonitz, “*Ab initio*,” *Phys. Rev. Lett.* **117**, 156403 (2016).
- [40] Tobias Dornheim, Simon Groth, Fionn D Malone, Tim Schoof, Travis Sjostrom, WMC Foulkes, and Michael Bonitz, “*Ab initio* quantum monte carlo simulation of the warm dense electron gas,” *Physics of Plasmas* **24**, 056303 (2017).
- [41] W. Kohn and L. J. Sham, “Self-consistent equations including exchange and correlation effects,” *Phys. Rev.* **140**, A1133–A1138 (1965).
- [42] J. C. Smith, A. Pribram-Jones, and K. Burke, “Exact thermal density functional theory for a model system: Correlation components and accuracy of the zero-temperature exchange-correlation approximation,” *Phys. Rev. B* **93**, 245131 (2016).
- [43] Miguel A.L. Marques, Micael J.T. Oliveira, and Tobias Burnus, “Libxc: A library of exchange and correlation functionals for density functional theory,” *Computer Physics Communications* **183**, 2272 – 2281 (2012).
- [44] Valentin V. Karasiev, Travis Sjostrom, James Dufty, and S. B. Trickey, “Accurate homogeneous electron gas exchange-correlation free energy for local spin-density calculations,” *Phys. Rev. Lett.* **112**, 076403 (2014).
- [45] Simon Groth, Tobias Dornheim, and Michael Bonitz, “Free energy of the uniform electron gas: Testing analytical models against first-principles results,” *Contributions to Plasma Physics* **57**, 137–146 (2017).
- [46] Travis Sjostrom and Jérôme Daligault, “Gradient corrections to the exchange-correlation free energy,” *Phys. Rev. B* **90**, 155109 (2014).
- [47] Valentin V Karasiev, James W Dufty, and SB Trickey, “Nonempirical semi-local free-energy density functional for warm dense matter,” *arxiv:1612.06226* (2017).
- [48] D J Carrascal, J Ferrer, J C Smith, and K Burke, “The hubbard dimer: a density functional case study of a many-body problem,” *Journal of Physics: Condensed Matter* **27**, 393001 (2015).
- [49] Aron J. Cohen and Paula Mori-Sánchez, “Landscape of an exact energy functional,” *Phys. Rev. A* **93**, 042511 (2016).
- [50] Johanna I. Fuks, Mehdi Farzanehpour, Ilya V. Tokatly, Heiko Appel, Stefan Kurth, and Angel Rubio, “Time-dependent exchange-correlation functional for a hubbard dimer: Quantifying nonadiabatic effects,” *Phys. Rev. A* **88**, 062512 (2013).
- [51] J. I. Fuks and N. T. Maitra, “Charge transfer in time-dependent density-functional theory: Insights from the asymmetric hubbard dimer,” *Phys. Rev. A* **89**, 062502 (2014).

- [52] Johanna I. Fuks and Neepta T. Maitra, "Challenging adiabatic time-dependent density functional theory with a hubbard dimer: the case of time-resolved long-range charge transfer," *Phys. Chem. Chem. Phys.* **16**, 14504–14513 (2014).
- [53] Volodymyr Turkowski and Talat S Rahman, "Nonadiabatic time-dependent spin-density functional theory for strongly correlated systems," *Journal of Physics: Condensed Matter* **26**, 022201 (2014).
- [54] Killian Deur, Laurent Mazouin, and Emmanuel Fromager, "Exact ensemble density functional theory for excited states in a model system: Investigating the weight dependence of the correlation energy," *Phys. Rev. B* **95**, 035120 (2017).
- [55] K. Burke, J. C. Smith, P. E. Grabowski, and A. Pribram-Jones, "Exact conditions on the temperature dependence of density functionals," *Phys. Rev. B* **93**, 195132 (2016).
- [56] Ebad Kamil, Robert Schade, Thomas Pruschke, and Peter E. Blöchl, "Reduced density-matrix functionals applied to the hubbard dimer," *Phys. Rev. B* **93**, 085141 (2016).
- [57] K. Schönhammer, O. Gunnarsson, and R. M. Noack, "Density-functional theory on a lattice: Comparison with exact numerical results for a model with strongly correlated electrons," *Phys. Rev. B* **52**, 2504–2510 (1995).
- [58] Attila Cangi, E. K. U. Gross, and Kieron Burke, "Potential functionals versus density functionals," *Phys. Rev. A* **88** (2013).
- [59] Attila Cangi and Aurora Pribram-Jones, "Efficient formalism for warm dense matter simulations," *Phys. Rev. B* **92**, 161113 (2015).
- [60] Weitao Yang, Paul W. Ayers, and Qin Wu, "Potential functionals: Dual to density functionals and solution to the v -representability problem," *Phys. Rev. Lett.* **92**, 146404 (2004).
- [61] Attila Cangi, Donghyung Lee, Peter Elliott, Kieron Burke, and E. K. U. Gross, "Electronic structure via potential functional approximations," *Phys. Rev. Lett.* **106**, 236404 (2011).
- [62] See Supplemental Material at [URL will be inserted by publisher] for a thorough derivation of the XC free energy equations and numerical demonstrations of the various approximations.
- [63] Ethan W. Brown, Bryan K. Clark, Jonathan L. DuBois, and David M. Ceperley, "Path-integral monte carlo simulation of the warm dense homogeneous electron gas," *Phys. Rev. Lett.* **110**, 146405 (2013).
- [64] Fionn D. Malone, N. S. Blunt, Ethan W. Brown, D. K. K. Lee, J. S. Spencer, W. M. C. Foulkes, and James J. Shepherd, "Accurate exchange-correlation energies for the warm dense electron gas," *Phys. Rev. Lett.* **117**, 115701 (2016).